Available online at www.sciencedirect.com
ScienceDirect
Surface Science 601 (2007) 4862–4872
SURFACE SCIENCE
www.elsevier.com/locate/susc

Metal interface formation studied by high-energy reflection energy loss spectroscopy and electron Rutherford backscattering

M. Vos *, M.R. Went

Atomic and Molecular Physics Laboratories, Research School of Physical Sciences and Engineering, The Australian National University, Canberra 0200, Australia

Received 25 June 2007; accepted for publication 31 July 2007
Available online 26 August 2007

Abstract

We demonstrate that high-energy, high-resolution reflection electron energy loss spectroscopy can provide unique insights into interface formation, especially for the case where an extended interface is formed. By changing the geometry and/or electron energy the electronic structure can be probed over a range of thicknesses (from 10s of Å to more than 1000 Å). At the same time one resolves the elastically scattered electrons into different components, corresponding to scattering of atoms with different mass (so-called 'electron Rutherford backscattering'). Thus these high-energy REELS/elastic scattering experiments obtain information on both the electronic structure and the atomic composition of the overlayer formed.

Keywords: Thin films; Reflection electron energy loss spectroscopy; Elastic electron scattering; Plasmon excitation

1. Introduction

Photoemission is one of the main tools used to study surface layers. Composition can be obtained from core level intensities and the electronic structure can be studied by measuring valence band spectra, or by studying details of the line shape/satellite structures of the core levels. With the advent of synchrotron radiation it became possible to vary the probing depth by tuning the outgoing energies. If surface sensitivity is required one chooses the outgoing energies close to the minimum of the inelastic mean free path. Thicker layers can be studied by increasing the energy of the outgoing electrons. Nowadays, spectra with kinetic energy in the range of 5–10 keV are routinely obtained at the larger storage ring facilities [1]. Decreasing X-ray flux with increasing energy in combination with the decreasing photoexcitation cross section with energy makes any further increase of the probing depth by increasing the photoelectron energy a real challenge.

Reflection energy loss spectroscopy (REELS) has long been used to study the interaction of electrons with a surface, and is an important tool to help understand photoemission in general, as the latter necessarily involves the transmission of electrons from the material under investigation into the vacuum. REELS provides information about bulk and surface loss processes. Indeed by comparing REELS spectra taken at different energies one can determine both the surface and bulk loss functions (see e.g. [2]). At very high energies the surface loss contribution to the spectra becomes rather minor. In this paper we present REELS spectra taken at energies up to 40 keV. As the mean free path of electrons increases with energy this allows us to probe rather thick layers. Here we want to demonstrate that high-energy REELS can be used as an in-house technique to study the electronic structure of thick layers. It is in this sense an alternative to high-energy photoemission, and is a method that could quite easily be adapted to even higher energies.

By comparing the loss functions obtained by high-energy REELS with bulk loss functions, as known from transmission EELS measurements and optical measurements, we

* Corresponding author.
E-mail address: maarten.vos@anu.edu.au (M. Vos).

0039-6028/$ - see front matter © 2007 Elsevier B.V. All rights reserved.
doi:10.1016/j.susc.2007.07.031

want to show experimentally that this technique is only affected in minor ways by surface effects. Subsequently we will show examples of interface formation by deposition of an Al film on several substrates (Mo, Pt and Au). Aluminum is chosen as it has a simple energy loss spectrum dominated by a plasmon peak. The energy loss spectra of Mo, Pt and Au are more complicated, but all have characteristic features, easily resolved with our spectrometer. Can the spectra obtained from an overlayer system be described, at least in first-approximation, as a linear combination of the substrate spectra and the overlayer spectra? We will see that this sometimes is the case, but often not. Often Al reacts with the substrate and an extended interface is formed. By adding Al in subsequent evaporations we can establish at what point pure Al forms, as is evident of the appearance of the Al plasmon. This signals the end of the interface formation. It can happen for surprisingly large Al layer thicknesses (several 100s of Å), and the bulk sensitivity of this technique is thus very beneficial. High-energy REELS is thus shown to be a good technique to obtain information on thick layers (at least by conventional electron spectroscopy standards).

Interest in investigating the possibilities of these high-energy REELS measurement was triggered in part by the realization that the elastic peak splits up at high energies in different components, corresponding to electrons scattering of atoms of different mass [3]. This is because if an electron is scattered over a large angle, it transfers a significant amount of momentum to the scattering atom. If the momentum transferred to the atom is **q**, then the corresponding (mean) recoil energy E_r, transferred from the electron to the atom is given by

$$E_r = q^2/2M \tag{1}$$

with M the mass of the atom. The magnitude of E_r for the element studied in the paper is given in Table 1 together with other scattering properties. The electron energy will be reduced by this amount. Thus, in favorable cases, the elastic peak splits up into different components, due to scatterers with different mass M and the measured structure can be used to determine the surface composition. This technique is then often referred to as 'electron Rutherford backscattering' (ERBS) (see e.g. [4]), as it resembles (ion) Rutherford backscattering in many ways. REELS at high energies provides complimentary information, mainly on the electronic structure, that is obtained simultaneously with ERBS data. In spite of the different acronyms the ERBS experiment is identical to a REELS experiment taken at high energies. In REELS one obtains information of the part of the spectra that is due to electronic excitations *in addition* to elastic scattering, in ERBS one considers the (quasi-)elastic peak only. Sometimes, as we will see, one has also to consider the influence of the recoil energy on the shape of the energy loss structures [5].

The first attempts to use ERBS as an analytical tool were made, not surprisingly, for the case of hydrogen, as, due to its small mass, the recoil energy for protons is relatively large. At high energies, using Rutherford cross sections, there were systematic deviations from the expected and observed H peak area [8]. At lower energies, with the H peak only partly resolved, Yubero et al. used empirical cross sections obtained from the measurements of various plastics to determine the H concentration in amorphous carbon films, and they obtained reasonable agreement with ion beam analysis results [9]. By increasing the energy and scattering angle it became possible to separate many more elements. For example we could separate Si from O, S from Mo, etc. [4]. On the other hand, when studying samples containing e.g. Fe and Au, then the Fe peak is only partly resolved. Even when studying well-defined compounds the observed elastic peak intensity often deviates by 20% from the expected values [4]. Thus interpretation of ERBS data on a fully quantitative level is still in its infancy. Interpretation for reactive overlayer systems is even more complicated than for stoichiometric compounds [10], as in this case the thickness of the overlayer and reacted layer, as well as their inelastic mean free path are required.

Table 1
Various calculated quantities pertaining to elastic scattering for different elements at different incoming energy E_0

Element	E_0 (keV)	E_r 120° (eV)	$\frac{d\sigma}{d\Omega}$ 120° (Å^2)	λ_{el} (Å)	λ_{tr} (Å)	λ_{in} (Å)
Al	5	0.30	1.70×10^{-4}	40	4950	88
Mo	5	0.09	2.12×10^{-3}	15	319	59
Pt	5	0.04	3.02×10^{-3}	13	147	41
Al	20	1.24	1.00×10^{-5}	170	21,900	288
Mo	20	0.35	1.37×10^{-4}	39	2590	190
Pt	20	0.17	5.95×10^{-4}	28	980	131
Al	40	2.53	2.44×10^{-6}	307	74,000	528
Mo	40	0.71	3.32×10^{-5}	64	7950	346
Pt	40	0.35	1.70×10^{-4}	42.2	2800	237

The recoil energy E_r was obtained from Eq. (1). The differential elastic scattering cross section $\frac{d\sigma}{d\Omega}$ at 120° and 40 keV was obtained from the ELSEPA package [6] and so was the elastic mean free path $\lambda_{el} = 1/N\sigma_{el}$ (with N the atomic density and σ_{el} the total elastic cross section) and the transport mean free path λ_{tr}. The inelastic mean free path λ_{in} was obtained from the TPP formula [7].

There is a strong dependence on the elastic cross section on the atomic number (it scales roughly with Z^2). For overlayer systems this means that the probing depth can vary greatly, depending on the elemental depth distribution [11–13]. For some of the cases studied here the probing depth is much larger than the inelastic mean free path. In this paper we will restrict ourselves to semi-quantitative interpretation of the elastic part of the spectrum, mainly to discuss the probing depth in these experiments.

High-energy EELS spectra are usually taken in a transmission geometry. This technique was developed into a fine art the 1960s and remarkable energy resolutions were obtained (e.g. 50–80 meV at 50 keV [14]). It then became integrated in the electron microscope, and is nowadays one of the main techniques in quantitative electron microscopy [15]. EELS in a reflection geometry is usually done at $\simeq$1 keV energy with modest resolution ($\simeq$1 eV). REELS Measurements up to 10 keV were reported by Tougaard

and Kraaer [16]. REELS spectra are usually taken from single element targets in a reflection geometry.

In this paper we want to start exploring the possibilities of REELS at higher energies (up to 40 keV) with reasonable resolution (0.5 eV) for the study of interface formation. We give examples of reactive and non-reactive interfaces, and show that this technique probes rather thick layers. We will show that by collecting the REELS and the ERBS spectrum in one measurement this approach probes both the electronic structure and the atomic composition of the near surface layer. With increasing understanding of both ERBS and high-energy REELS experiments, the unique complimentary nature of the ERBS and REELS data, that are obtained simultaneously, should make a fully quantitative study of extended interface formation possible.

2. Experimental details

The main spectrometer is shown in Fig. 1. The spectrometer is equipped with two electron guns. Each gun emits electrons with 500 eV energy. The sample is surrounded by a high voltage sphere kept between 4.5 keV and 39.5 keV. Thus electrons with energies between 5 keV and 40 keV are scattered from the sample. Drift and ripple of the (5–40 keV) high voltage power supply do not affect the energy resolution of the experiment as the potential that accelerates the electron when entering the high voltage sphere is the same as the potential that decelerates the electrons when leaving the high voltage sphere. After being decelerated and focussed by a slit lens stack the electrons enter a hemispherical analyzer. The entrance element of this lens stack is at the high voltage sphere potential. The pass energy of the hemispherical analyzer was 200 eV. A two-dimensional detector was used allowing electrons in an energy window of 30 eV to be detected simultaneously.

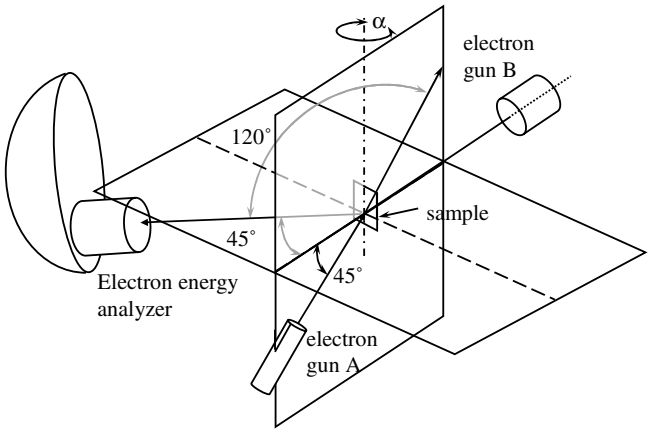

Fig. 1. An overview of the experimental configuration. If gun A is used the sample is positioned as shown and the scattering angle is 120°. Angle between the sample surface normal and incoming and outgoing trajectories is then 45° (but surface normal, incoming and outgoing trajectories are not in the same plane). If gun B is used (scattering angle 45°) the sample is rotated over angle α by 112.5°. The incoming and outgoing trajectories are now more glancing (both 67.5° with the surface normal).

For more details about the analyzer and high voltage sphere design see Ref. [17], a more detailed drawing of the lens stack optics is given in Ref. [18]. Data were taken with current less than 1 nA. Typically a spectrum was obtained over a 2-h period. Pressure in the main chamber was $\simeq 1.0 \times 10^{-10}$ torr during the measurement. Deteriorated of the sample over time was noticed only for Mo when measured over a 24 h period.

Samples were prepared in situ by sputtering using Xe^+ ions. While sputtering a CMA was used to monitor the REELS spectra taken at 1–2 keV. Sputtering was terminated when the measured REELS spectra no longer changed. Auger spectra taken after cleaning revealed no C or O at the surface. The sample was then transferred under UHV to the main spectrometer for the high-energy REELS measurements.

For evaporation the sample was transferred to a dedicated evaporation chamber. Aluminum was deposited by thermal evaporation from a boron carbon nitrite composite crucible. The sample was positioned on a magnetic transfer arm 30 cm away from the evaporator. Power in the evaporator was 280 W. As the thermal conductance of the sample was not ideal, some rise in temperature of the sample is expected. To test the sample heating by the evaporator we did a dummy run with a thermocouple attached to the sample (hence making it impossible to transfer this sample in the main spectrometer). A temperature rise of 60 °C was found for a short evaporation (10 Å of Al) increasing to 100 °C for evaporation of several 100s Å of Al. Thus we want to stress that the interface reactions studied here are characteristic for the interface at a slightly elevated temperatures. Sometimes the sample was investigated as well with the 1–2 keV CMA after Al deposition.

3. Results

3.1. REELS of homogenous materials

Aluminum with its sharp plasmons and well-established surface plasmon is often used as a prototypical test case to establish the spectrometer performance. In Fig. 2 we show a spectrum of an evaporated Al film measured with gun A (see Fig. 1) at 40 keV and a spectrum obtained at 5 keV using gun B. This corresponds to the most bulk-sensitive measurement condition and the most surface sensitive measurement condition, employed in this paper. Indeed in the surface sensitive measurement the surface plasmon, near 10 eV energy loss, is about half the intensity of the bulk plasmon (near 15 eV). The spectra were corrected for multiple loss features using the procedure described by Tougaard and Chorkendorff (TC) [19] and in this way we obtain the normalized differential inelastic mean free path (DIIMFP). For surface sensitive measurement the DIIMFP shows a large peak near 10 eV, and negative intensities near 25 eV. Both are a well-known consequence of the surface excitations, not accounted for in the TC procedure. The TC procedure treats the surface excitation as a bulk feature, and as

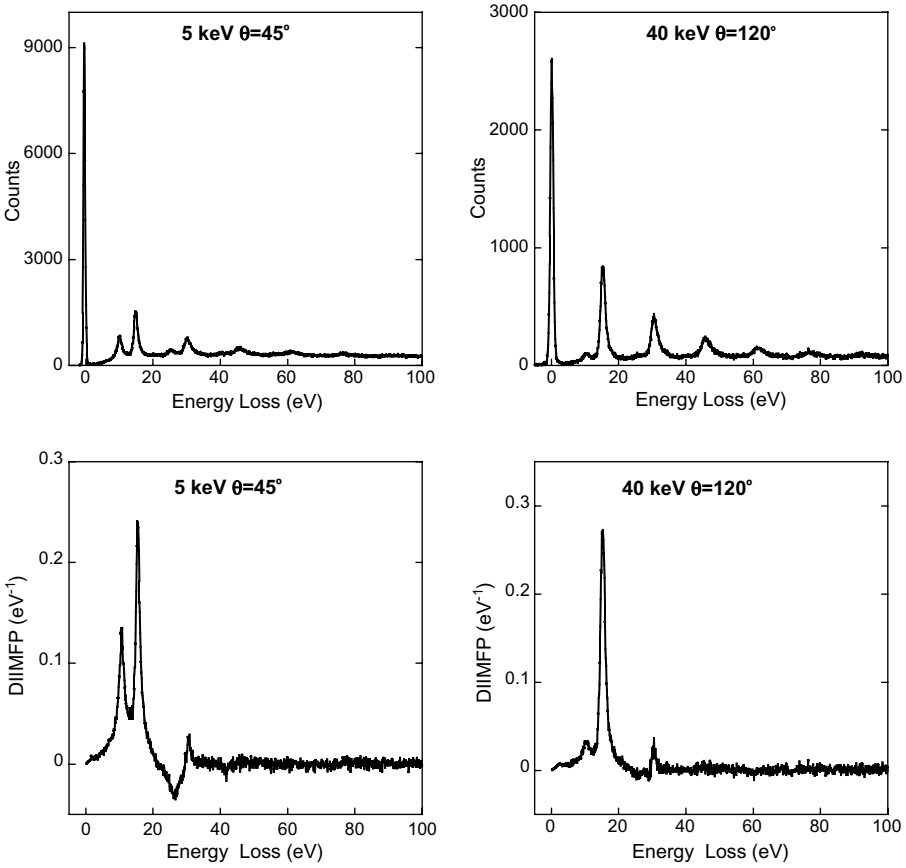

Fig. 2. Measurement of Al REELS under the most surface sensitive conditions (left, 5 keV, using gun B) and the most bulk-sensitive conditions (right, 40 keV, using gun A). The top panels show the raw data, the lower panel shows the loss function, as derived using the Tougaard–Chorkendorff procedure [19].

a consequence overestimate the intensity due to excitation of both a surface and a bulk plasmon that is evident in the spectra near 25 eV energy loss. The DIIMFP taken at high energies is much less affected by these effects (as the surface plasmon excitation probability is less), and it approached the Al bulk loss function much closer.

There is a small peak near 30 eV energy loss. It is as clearly visible in the DIIMFP obtained at 5 keV, as the one obtained at 40 keV, and hence we do not think it is a consequence of surface effects. The fact that part of the second plasmon survives the TC multiple scattering correction procedure indicates that the intensity of the second plasmon exceeds that expected for a Poisson distribution, and can be interpreted as a sign of direct double plasmon excitation. This process was predicted by Ashley and Ritchie [23], and similar conclusions were reached from transmission EELS measurements [24].

Now let us have a look at the REELS spectra of the materials used as a substrate in this paper. All these materials show after sputter-cleaning a feature-rich REELS spectra. For Mo, Pt and Au we show these spectra in Fig. 3 taken at 40 keV in the bulk-sensitive geometry (using electron gun A). The spectra were again corrected for multiple loss features using the TC procedure [19], as shown in the lower panels of Fig. 3. This approach should be quite good as the contribution of the surface plasmons should be small under these condition. For Pt and Au the results are compared with those obtained from transmission measurements as published by Daniels et al. [21]. As a different multiple scattering procedure was followed for the transmission measurements we can only compare the relative intensity, and the vertical scale of the transmission measurement was adjusted for easy comparison. At high-energy loss values the agreement is good, at low loss values the REELS results show relatively more intensity. This is attributed to surface excitations that contribute more in the REELS experiment compared to the transmission one. Transmission EELS spectra are, to our knowledge, not available for Mo, however our spectra show good resemblance with bulk energy loss features obtained from optical measurements [20]. For Au a more detailed study of decomposition of the spectra in surface and bulk energy loss contributions will be published elsewhere [25].

3.2. REELS of overlayer–substrate systems

In the previous section we showed that, especially at high energies, the REELS spectrum resembles the bulk loss function of the material under investigation. Now we want to investigate if we can use REELS for overlayer–substrate

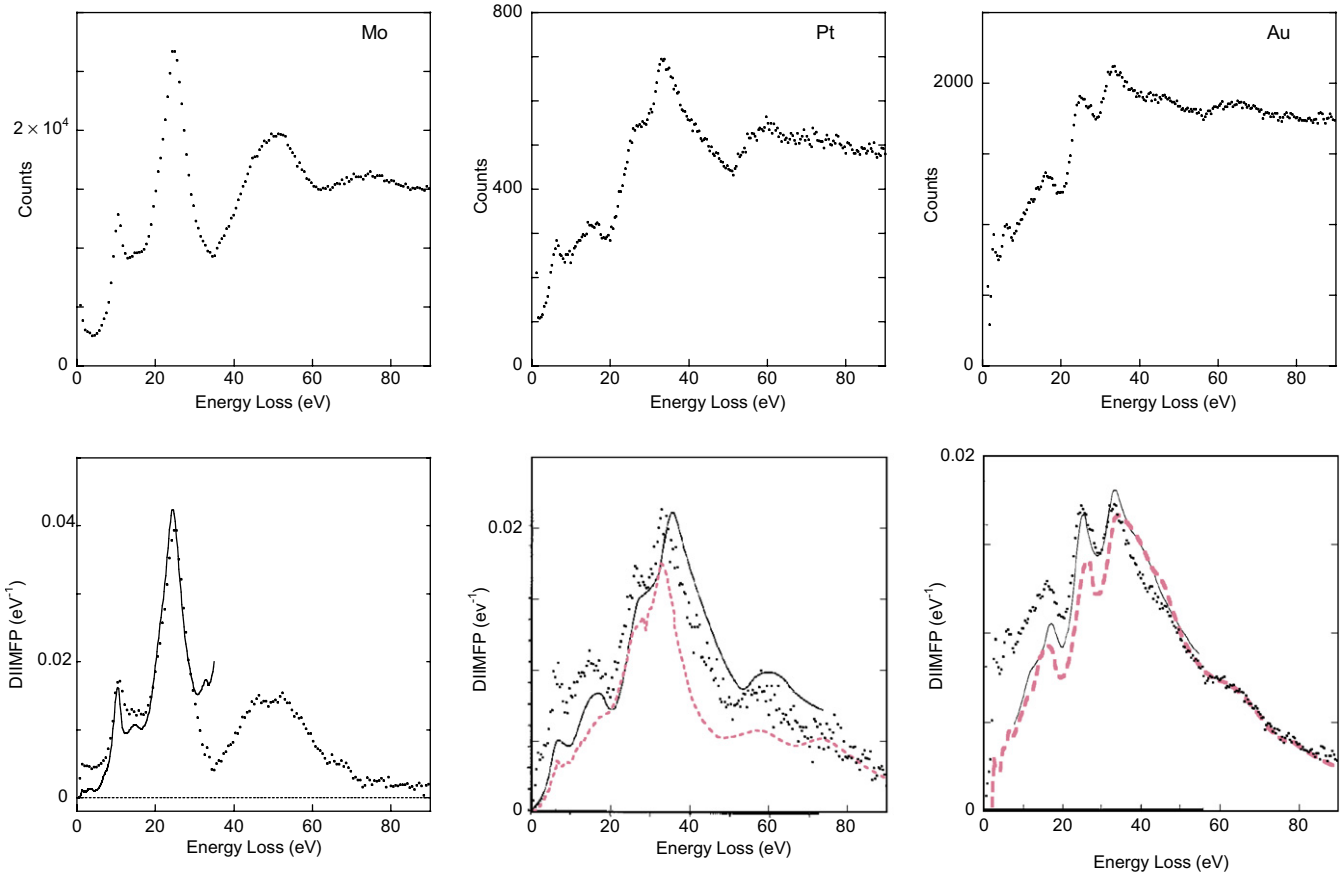

Fig. 3. The raw REELS spectra obtained at 40 keV of Mo Pt and Au (top panels). The effect of multiple inelastic excitations is removed in the lower panel, and the results are compared with those obtained from optical measurements (Mo) by Weaver et al. [20] (solid line) and transmission EELS measurements (Pt, Au) by Daniels et al. [21] (solid lines). The dashed line in the case of Pt and Au is the (scaled) loss function derived from optical measurements as given by Palik [22].

systems. In REELS one measures the energy distribution of the electronic excitations for an electron backscattered from a material. This distribution is a signature of the electronic structure. In an substrate–overlayer system one can identify two or more phases (overlayer, substrate and possibly one or more phase formed at the interface), each with its own electronic structure and hence loss function. By monitoring the structures of the loss function as a function of overlayer thickness we can probe which phases are present in the sample.

The simplest case is where no reaction occurs, and the evaporated layer grows in a layer-by-layer mode. From the work of Kolaczkiewicz et al. it is known that Al grows (at low coverages) on Mo in a layer-by-layer mode, and that the system is stable for annealing up to 200 °C [26]. We show spectra of Mo covered with thick (by electron spectroscopy standards) Al layers (40 Å and 80 Å) (Fig. 4). The spectra were, for convenience, normalized in such a way that they largely overlap for large energy loss values. For the Mo substrate the main effect of Al deposition is a sharp peak at 15.2 eV energy loss relative to the Mo elastic peak. 15.2 eV corresponds to the plasmon energy and this feature is thus attributed to electrons scattering from Mo for which either the incoming or outgoing electron excited an Al plasmon. The main features of the Mo energy loss spectra are still discernable. Thus the measured energy loss spectra for the Al/Mo system can be described, at least in first-approximation, as the sum of a Mo REELS spectrum and an Al REELS spectrum. Taking the difference of the spectra before and after Al deposition we see that the excess intensity corresponds to the energies of the Al plasmon and Al surface plasmon. In the lower panel we show the spectra taken with a 'conventional' CMA using 1.5 keV electrons. Before deposition the spectrum resembles that reported for Mo by Chen et al. [27]. After deposition the Al plasmon starts dominating and no clear signature of the Mo substrate is observed, as expected as the evaporated layer thickness is much larger than the electron's inelastic mean free path at 1.5 keV (≃23 Å [7]). The second bulk plasmon, however still increases intensity going from a 40 Å layer to a 80 Å layer.

The behavior of Al deposition on Mo contrasts strongly with that seen for Al deposition on Pt. This system is known to form a surface alloy for thin layers at room temperature [28]. At somewhat elevated temperatures (150–220 °C) a solid state amorphization reaction has been observed for thicker layers [29]. Our Pt results are shown in the right panel of Fig. 4. Now no sign of an Al plasmon is found. Above

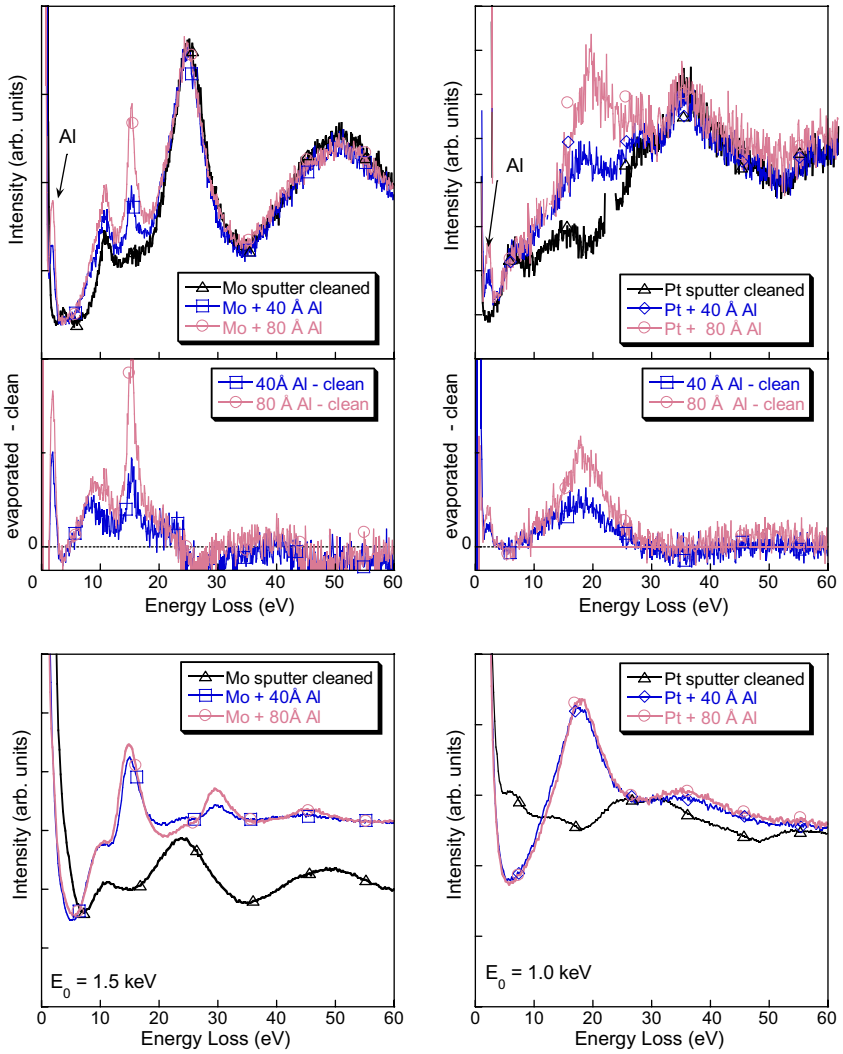

Fig. 4. A comparison of the raw (40 keV) REELS data obtained for Al deposition on Mo and Pt. For the Mo case the Al plasmon is clearly visible at the lowest coverage. However for Pt this is not the case. The difference between of the high-energy spectra before and after deposition (middle panels) has a strong correlation with the low energy REELS data taken from the same sample (lower panel). The structure appearing after evaporation near 2 eV energy loss is the Al elastic peak.

30 eV energy loss and below 10 eV energy loss the features of the Pt loss function still stands out. From the difference spectrum it is clear that the excess intensity is centered around 20 eV energy loss in a much broader peak (in comparison to the Al plasmon width). Increasing the coverage increases the difference before and after deposition, but the position and width of the peak in the difference spectrum does not change dramatically. We take the difference to be the rough shape of the loss function of an interface compound that is formed. Traditional REELS spectra collected at 1 keV seem to confirm this picture. Before Al deposition the spectrum resembles the Pt REELS spectrum published by Werner at 1 keV [30]. After 40 Å Al deposition the main feature resembles the difference spectra of the high-energy REELS experiment. The low energy REELS spectrum after 80 Å Al deposition is virtual indistinguishable from that after 40 Å Al deposition.

At very small energy loss ($\simeq$2 eV) an additional peak appears after Al deposition in the 40 keV REELS spectra. It is due to electrons scattering elastically from Al, rather than Pt or Mo. These electrons appear at a different energy as the energy transferred due to the recoil: $q^2/2M$ is larger for lighter atoms (see Table 1). Its separation from the main elastic peak is somewhat larger in Pt than in the Mo case. In these plots we aligned the zero loss of Pt and Mo with 0 eV, as is traditionally done in REELS, however when taking into account the recoil energy for scattering of Pt or Mo, then the actual position is at 0.35 eV and 0.71 eV. If the main elastic peak is aligned in that way, then the new feature is, within the measurement accuracy, at the recoil energy of Al (2.53 eV), confirming our interpretation of the origin of this peak. This is thus not an additional inelastic energy loss feature, but a feature that is part of the ERBS spectrum.

This Al peak appears, for identical coverage, more intense for evaporation on Mo, compared to that on Pt. This is not surprising as the Pt elastic cross section is much larger than the Mo elastic cross section, and the REELS sig-

nal strength is, at least in first order, proportional to the elastic cross section (as all detected electrons have been scattered elastically). Hence the relative strength of the Al peak after 40 Å and 80 Å deposition is larger for the Mo substrate compared to the Pt substrate.

It is clear that the Al–Pt interface forms a reacted layer. To further investigate the extent of this reaction additional Al layers were evaporated on the substrate. In Fig. 5 we show the Pt REELS spectra for Al coverages between 0 Å and 600 Å. Now we use two energies for the incoming electrons: 20 keV and 40 keV. At 80 Å coverage the 20 keV measurement has more intensity around 20 eV energy loss, i.e. it is intermediate between the 1 keV REELS measurement and the 40 keV REELS measurement. The difference between the 20 keV and 40 keV measurement decreases when going to 150 Å and 300 Å coverage. Now both measurements probe almost exclusively the reacted layer, and the substrate Pt contribution becomes small. At 300 Å the 40 keV measurement shows a clear shoulder near 15 eV energy loss (the Al plasmon energy), and the 20 keV spectrum shows even a distinct peak at this energy loss. Thus Al metal starts forming at this thickness. The intensity of this plasmon increases strongly with further Al deposition, and even the surface plasmon, second and third bulk plasmon become visible. These features develop again somewhat slower in the 40 keV measurement compared to the 20 keV measurement, due to the larger probing depth in the former case.

Let us focus on the elastic peak region in this coverage range. In Fig. 6 we show the 150 Å and 600 Å cases as an example. At 150 Å coverage it is possible to get a good fit using two Gaussians separated by the calculated difference in recoil energy. However the area obtained from these fits depends very much on the background choice (we used a Shirley background for these fits). The situation has changed at 600 Å. Not only has the Al signal strength increased, but the Pt signal has become weaker due to attenuation in the Al layer (the latter is evident from the

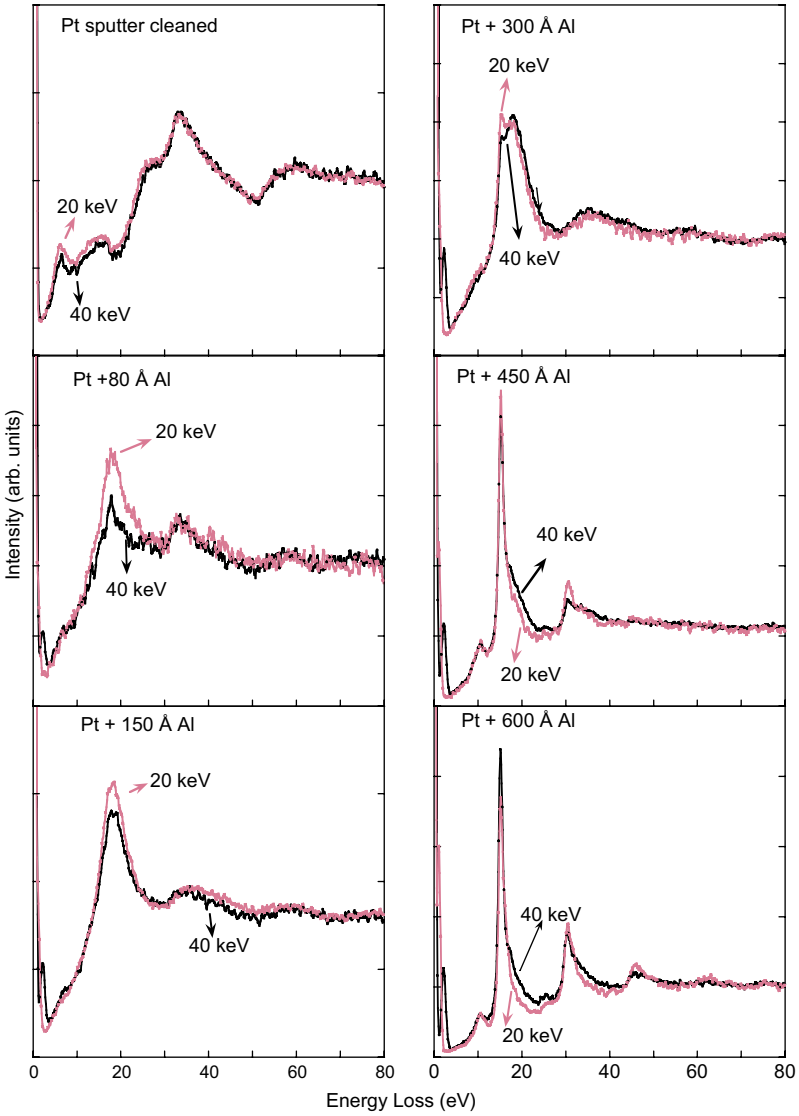

Fig. 5. Spectra taken at 40 keV and 20 keV incoming energy in a bulk-sensitive geometry for a Pt sample covered with increasing amount of Al.

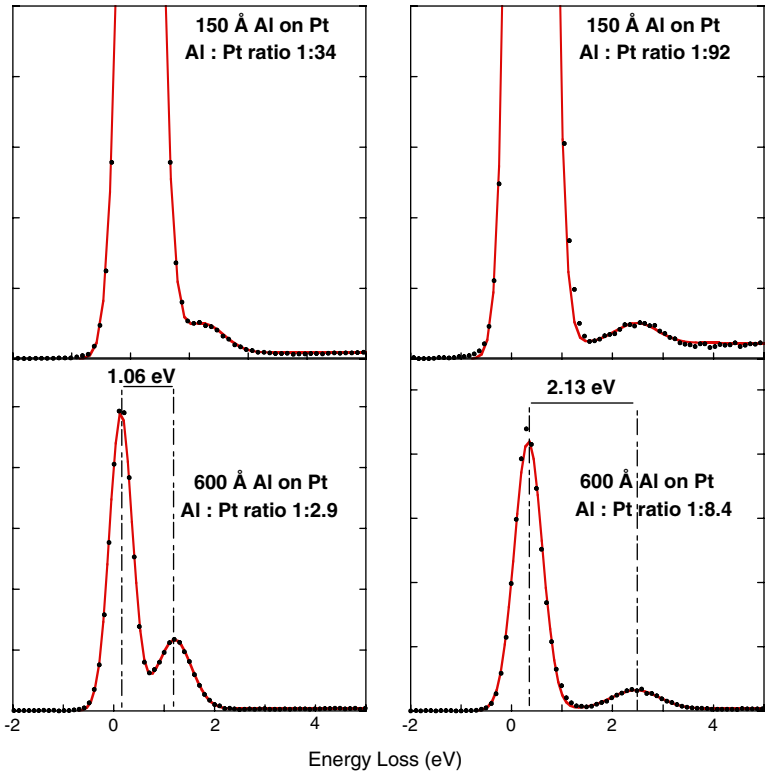

Fig. 6. Elastic region of the spectra taken at 150 Å and 600 Å Al coverage taken with gun A using a 20 keV (left panels) and a 40 keV (right panels) electron beam. The full line is a fit using two Gaussian peaks and a Shirley background. The main peak was aligned with the calculated recoil energy of Pt under these conditions.

decrease of the total count rate in the elastic peak area for a given beam current). Now the peak separation can be left free in the fit, and indeed values very close to those calculated from the recoil energies in Table 1 are obtained, further confirming our interpretation of this feature at low energy losses. This also suggest that the single-scattering approximation is valid, ie the electrons are deflected over a large angle by one collision only. The single-scattering approximation is expected to work well if the transport mean free path is much larger than the inelastic mean free path (see Ref. [31] for an explanation of the transport mean free path). This is indeed the case, esp. at high energies, as can be seen in Table 1. The relative intensity of the Al peak in the 20 keV measurement is stronger than in the 40 keV case, as at lower energy attenuation in the Al layer is stronger, and the thickness of the Pt layer that contributes effectively to the elastic peak is less.

There is a significant tail at the high-energy loss side of the Al plasmon, even at the highest coverage. This tail is more pronounced in the 40 keV measurement. This is in part due to the interface layer still contributing to the spectrum, but there is an additional reason for this shoulder at the high-energy loss side of the plasmon. This we illustrate in Fig. 7, for Al deposited on both Mo and Pt for a thickness range between 600 Å and 1500 Å. This is a different run, in which the Mo and Pt samples were mounted side-by-side, and hence the Al evaporated thickness should be virtual identical for both samples. In this thickness range the Mo and Pt elastic peak becomes attenuated severely, and the Al elastic peak, separated from the Pt, Mo elastic peak due to the difference in recoil energy, slowly starts dominating the spectra. To emphasize this we plotted the spectra in such a way that the elastic peak position corresponds to the recoil energy. At 600 Å the Al elastic peak is already more intense than the Mo elastic peak, but in the Al-on-Pt case the Pt elastic peak is still the largest. There are two reasons for this, the Pt differential elastic scattering cross section is about five times larger than the Mo one (see Table 1), and the Pt interface is not abrupt, Pt atoms are initially incorporated in the overlayer film, and hence the attenuation of the Pt signal by the Al layer is not as effective as in the case of Mo.

More interestingly, the plasmon peak of Al appears split as well. Each of the two components are separated by 15.2 eV (the Al plasmon energy) from either of the elastic peaks. Thus the cause of the splitting of the plasmon peak is clear. One is from electrons elastically scattered from Pt/Mo in combination with a plasmon excitation in the Al layer, the other is due to electrons scattered elastically from Al in combination with an Al plasmon creation event. The same splitting, somewhat less resolved, is seen for the second plasmon. Note also the unusual large intensity of the energy loss structures relative to the elastic peak in these experiments. This is also an indication that a large part of the electrons originate from deep in the target, and hence there is a large probability that these electrons create a

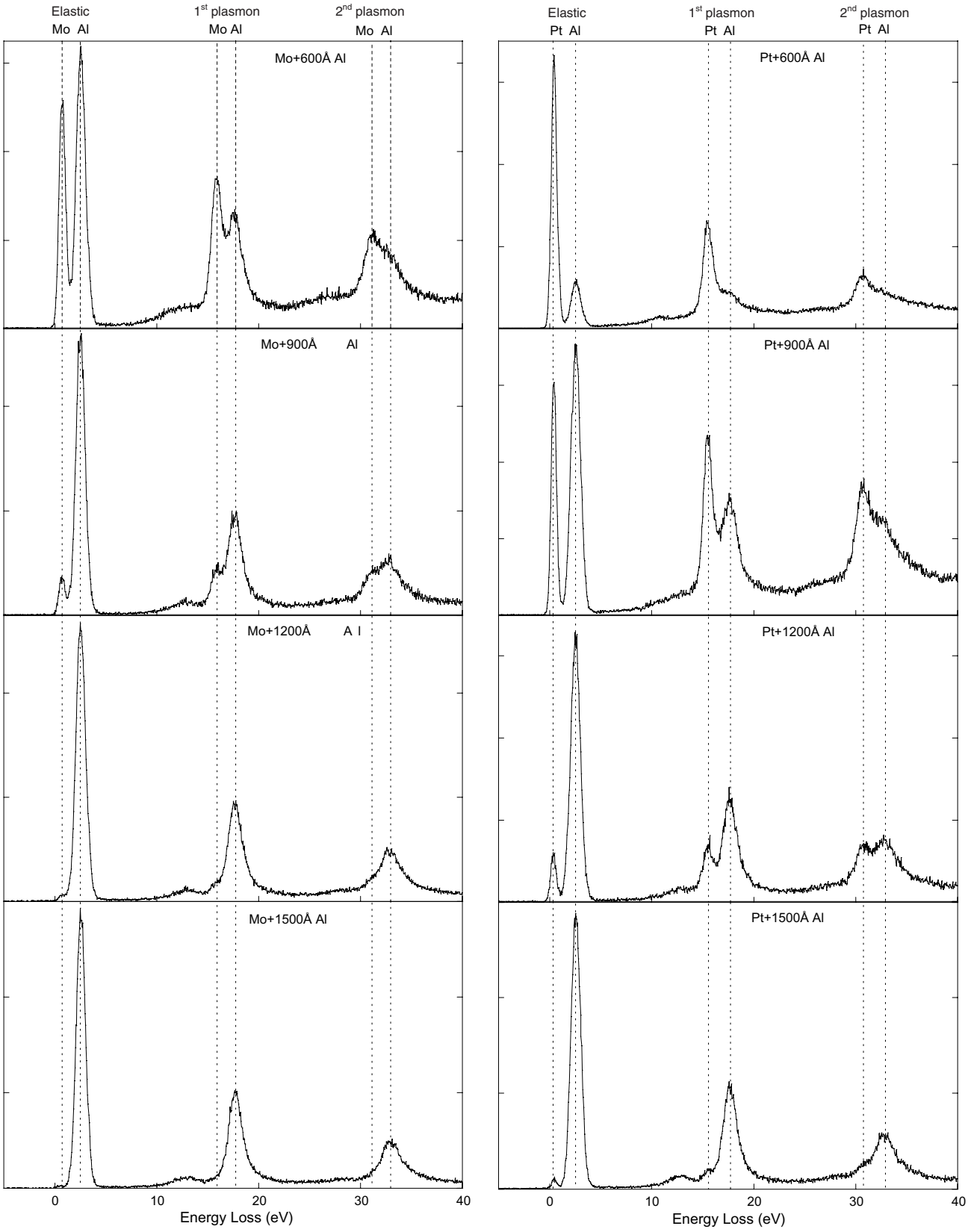

Fig. 7. The spectra, obtained using 40 keV electrons, from a Mo film and a Pt film covered with rather thick Al layers. Both the main elastic peak and the plasmon peaks are split into two components, due to the difference in recoil energy for scattering from a heavy (Pt, Mo) atom and a light (Al) atom.

plasmon. Large probing depth for light overlayers on heavy substrates were predicted, based on simulations by Zommer [12]. For the largest coverages the intensity in the loss area becomes more typical for Al films, and a

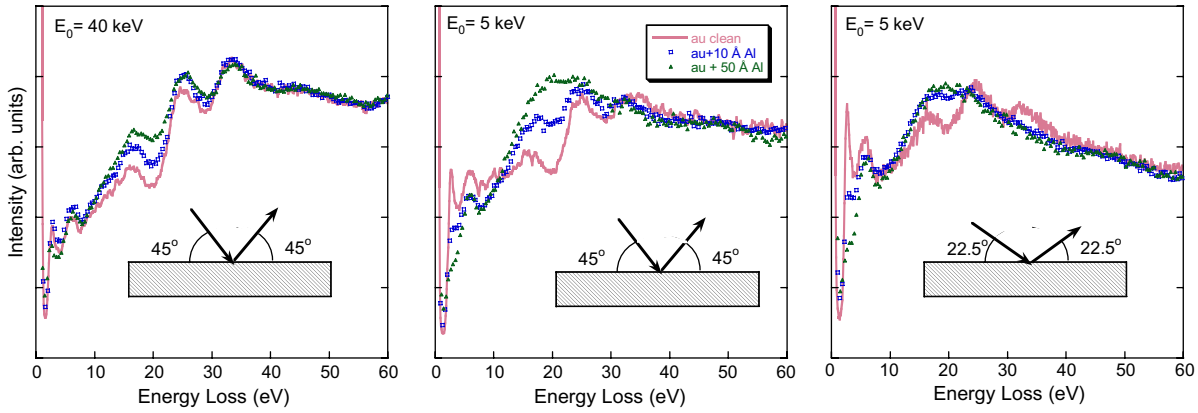

Fig. 8. Spectra of a Au substrate before and after Al deposition at energies and geometries as indicated. The surface loss peak clearly visible in the 5 keV measurements near 2.6 eV disappears after Al deposition. The spectra changes more rapidly with increasing surface sensitivity of the experiment, but no sign of the presence of pure Al metal is seen in any of the spectra (the legend displayed in the central panel applies to all panels).

one-component elastic peak and a one-component plasmon peak are observed. For a more quantitative analysis of the plasmon splitting see [5].

Finally we look at the interface between Al and Au. For this interface formation of a reacted layer continues for quite thick Al depositions. To look at the sample in more detail we utilize different energies and geometries. In our spectrometer it is possible to further vary the depth studied, without affecting the resolution, by lowering the energy and changing the geometry. Changing the geometry is possible by the use of an additional gun at a scattering angle of 45°, and in this case the incoming and outgoing beam are more glancing. We use rather low coverages (10 Å and 50 Å) of Al on a Au substrate as an example. The dramatic effects on the REELS spectra can be seen in Fig. 8. The shape of the bare Au spectrum changes with energy and geometry, as surface excitations become more prominent at lower energy/more glancing angle. This is evident by the increased intensity of the clean Au spectra between 0 eV and 10 eV energy loss. Deposition of Al reduces the peak at 2.5 eV, but surprisingly, the peak near 5.5 eV is much less affected. The main Au features are still well visible in the high-energy spectra taken in a bulk-sensitive geometry. On the other hand in the low energy spectra, taken in a surface sensitive geometry the spectra at 10 Å and 50 Å Al coverage are almost indistinguishable (but do not resemble at all the REELS spectrum of either Al or Au). Only the 5.5 eV feature seems unaffected in this geometry, suggesting that it is a feature present in both Au and the surface compound formed. The 5 keV spectra taken in a bulk-sensitive geometry behave in between these extremes. After 10 Å Al deposition the Au features are still clearly visible, but after 50 Å Al deposition the spectra resemble those taken in the surface sensitive geometry.

The interface formation continued always for many 100s of Å of Al deposition, but very poor reproducibility was found for the deposition thickness for which the Al plasmon is observed, the signature for the formation of a metallic Al layer. This is attributed to variations of the sample temperature reached during evaporation. This problem is not too surprising, as even at room temperature the solid state Al/Au reaction is known to continue over an extended period of time (years) [32] and reactions between Al and Au are infamous for causing failures in metal connections on chips (the so-called 'purple plague', see e.g. [33]). Better control of the sample temperature, during evaporation, is required if one wants to use this method for understanding the thermodynamics of this case of interface formation.

4. Conclusion and outlook

We have described high-energy reflection electron energy loss experiments and confirm that these experiments are bulk-sensitive. This has been a very exploratory research, more focussed on establishing possibilities rather than systematic experiments. The loss functions derived from the spectra of clean surfaces using the TC formalism compare well with those obtained from transmission EELS measurements or optical data. Interfaces formed by evaporation of Al on the substrates were monitored by REELS over a large range of overlayer thicknesses using a range of energies and two geometries. Thus one can vary the depth probed, and the picture obtained in this way gives clear insights in extended interface formation. Besides the dramatic changes in the REELS spectra it was found that deposition of Al on high Z substrates results in a splitting of the elastic peak, due to recoil effects. This splitting gives us a handle on the elemental composition of the probed layer. Recoil effects are clearly visible in the shape of the Al plasmon. In general, the spectra are all very dependent on the electron energy and geometry, but, at least qualitatively, the spectra can be interpreted as the sum of the bulk loss functions of the materials that contribute (overlayer, substrate and reacted layer). Changes due to energy and geometry variations are then a simple consequence of a variation in probing depth. Hence it is clear that REELS at high energies is often a very convenient way of probing

surface elemental composition as well as the electronic structure up to considerable depth ($\simeq$1000 Å in favorable cases). A prerequisite for this method is that the energy loss spectra of the overlayer and substrate have well-resolved distinguishing features.

Using modern two-dimensional detectors the signal strength is sufficient to acquire a spectrum over a broad range of energies 100 eV) in a few hours. The maximum depth we can probe is currently limited by the maximum energy (40 keV) obtainable in the spectrometer. A significant increase of the energy is not possible in our spectrometer, due to voltage breakdown problems, but the design of a spectrometer that can operate at higher energies should not pose unsurmountable problems. Cross sections will decrease with increasing energy, but this effect can be compensated for by increasing the beam current, now around 1 nA. At larger energies separation of the elastic intensity in different components becomes easier as the separation increases proportional to the primary energy used. Doppler broadening of the recoil energy (due to vibrational motion of the atoms [3]) will set a lower limit, however, for the peak width of any structure that can be observed. This Doppler broadening will increase with the square root of the primary energy, and this effect will be most noticeable for scattering from low Z targets. Using this technique in a scanning microscopy would make spot-wise analysis of the electronic structure *as well as* the composition possible.

Acknowledgement

This research was made possible by a Grant of the Australian Research Council.

References

[1] J. Zegenhagen, C. Kunz (Eds.), Proceedings of the Workshop on Hard X-ray Photoelectron Spectroscopy – HAXPES, Nucl. Instrum. and Meth. A 547 (2005).
[2] W.S.M. Werner, Phys. Rev. B 74 (7) (2006) 075421.
[3] M. Vos, Phys. Rev. A 65 (2002) 12703.
[4] M. Went, M. Vos, Appl. Phys. Lett. 90 (2007) 072104.
[5] M. Vos, M. Went, J. Electron Spectrosc. Relat. Phenom. xx (in press) doi:10.1016/j.elspec.2007.05.003.
[6] F. Salvat, A. Jablonski, C.J. Powell, Comput. Phys. Commun. 165 (2005) 157.
[7] S. Tanuma, C.J. Powell, D.R. Penn, Surf. Interface Anal. 20 (1993) 77.
[8] C.A. Chatzidimitriou-Dreismann, M. Vos, C. Kleiner, T. Abdul-Redah, Phys. Rev. Lett. 91 (2003) 57403.
[9] F. Yubero, V.J. Rico, J.P. Espinos, J. Cotrino, A.R. Gonzalez-Elipe, Appl. Phys. Lett. 87 (2005) 084101.
[10] M. Went, M. Vos, R.G. Elliman, J. Electron Spectrosc. Relat. Phenom. 156–158 (2007) 387.
[11] L. Zommer, A. Jablonski, J. Electron Spectrosc. Relat. Phenom. 150 (2006) 56.
[12] L. Zommer, Surf. Sci. 600 (2006) 4735.
[13] M. Vos, M.R. Went, Surf. Sci. 601 (2007) 1536.
[14] J. Daniels, Z. Phys. 203 (1967) 235.
[15] R.F. Egerton, Electron energy-loss spectroscopy in the electron microscope, second ed., Plenum Press, New York, 1996.
[16] S. Tougaard, J. Kraaer, Phys. Rev. B 43 (2) (1991) 1651.
[17] M. Vos, G.P. Cornish, E. Weigold, Rev. Sci. Intrum. 71 (2000) 3831.
[18] M. Vos, V. Sashin, C. Bowles, A. Kheifets, E. Weigold, J. Phys. Chem. Solids 65 (2004) 2035.
[19] S. Tougaard, I. Chorkendorff, Phys. Rev. B 35 (13) (1987) 6570.
[20] J.H. Weaver, D.W. Lynch, C.G. Olson, Phys. Rev. B 10 (2) (1974) 501.
[21] J. Daniels, C. Festerberg, H. Raether, K. Zeppenfeld, Optical Constants of Solids by Electron Spectroscopy, Springer Tracts in Modern Physics, vol. 54, Springer, 1970, p. 77.
[22] E. Palik, Handbook of Optical Constants of Solids, Academic Press, New York, 1985.
[23] J. Ashley, R. Ritchie, Phys. Stat. Sol. 38 (1970) 425.
[24] P.E. Batson, J. Silcox, Phys. Rev. B 27 (9) (1983) 5224.
[25] W. Werner, M.R. Went, M. Vos, Surface plasmon excitation at a Au surface by 150–40,000 eV electrons, Surf. Sci. 601 (2007) L109.
[26] J. Kolaczkiewicz, M. Hochol, S. Zuber, Surf. Sci. 247 (1991) 284.
[27] T. Chen, Z. Zhang, Z. Ding, R. Shimizu, K. Goto, J. Electron Spectrosc. Relat. Phenom. 159 (2007) 62.
[28] K. Wilson, J. Brake, A.F. Lee, R. Lambert, Surf. Sci. 387 (1997) 257.
[29] B. Blanpain, L.H. Allen, J.-M. Legresy, J.W. Mayer, Phys. Rev. B 39 (18) (1989) 13067.
[30] W.S.M. Werner, Surf. Sci. 588 (1–3) (2005) 26.
[31] W.S.M. Werner, Surf. Interface Anal. 31 (2001) 141.
[32] Ž. Marinković, V. Simić, Thin Solid Films 75 (1981) 229.
[33] G. Chen, IEEE Interact. Parts, Mater. Packag. 3 (1967) 149.